

Modelling and Experimental Analysis for Performance Improvement of Photovoltaic Module using Different Cooling Systems

Alaa F. M. Ali ¹, Ola Mostafa A. Saleh ^{1,2}, Ashraf Nasr EL-Deen Mourad ³, Hamdy A. Ziedan ^{1,□}, and Essam Ali ¹



Abstract This paper will review, analyze, model, and check experimentally the most effective techniques of photovoltaic (PV) cooling and control of its temperature in general. This will be analyzed and discussed to choose the suitable methods for Middle East Countries, especially Egypt. Namely, it is well known that an increase in electrical efficiency is a direct result of any decrease in the panel temperature. Several cooling techniques will be studied, analyzed, modelled, and check experimentally the best based on active, passive water and air cooling, as these are the simplest techniques. Improving electrical efficiency depends mainly on the technique used in cooling, geographical position, type and size of the module, and the month or season of the year. Usually, the overall efficiency records improvement with a rise of 10-15 %. Finally, a comparison on deferent cooling techniques for PV panels will be made to discuss which type is suitable for Egypt.

Keywords: Modelling; experimental analysis; quality; photovoltaic cells; cooling systems; efficiency

List of Abbreviations

AE : Absolute Error.
 BM : Bisection Method.
 CFD : computational fluid dynamics.
 DDM : double-diode model.
 MAE : Mean Absolute Error.
 NRM : Newton-Raphson method.
 OF : Objective Function.
 PCM : with phase-change materials.
 PDMS: Poly-dimethyl siloxane.
 PV : Photo Voltaic
 PVT : photovoltaic thermal systems.
 SDM : single-diode model.
 RMSE : Root Mean Square Error.

List of Symbols

$\bar{I}_{(V_i, \xi)}$: The estimated current.
 I_{cell} : The cell current.
 I_{D1} and I_{D2} : are the currents passing through diodes.
 I_{pv} : The PV current.
 K : Boltzmann constant.
 N_s : number of series cells.
 N_p : number of parallel cells.
 q : charge of the electron.
 R_s : Series Resistance.
 R_p : Parallel Resistance.
 T : The panel temperature in Kelvin.
 T_{cell} : The cell temperature.
 V_t : The thermal voltage.

1 Introduction

In this industrial world, it is well known that fossil fuel is the primary basis of electricity production, especially in the developing countries. Based on the risks of fossil fuels, the use of sustainable sources of energy

Received: 26 July 2023/ Accepted: 29 August 2023

□ Corresponding Author: (H.Aziedan@aun.edu.eg)

1. Electrical Engineering Department, Faculty of Engineering, Assiut University, 71518 Assiut, Egypt; eng_alaa_farah86@aun.edu.eg; essam.ali@aun.edu.eg
2. Electrical Technology Department, Egyptian German College (EGC), Misr International Technological University (MITU), Assiut, Egypt; ola.mostafa@itecassiut.edu.eg
3. Upper Egypt Electricity Production Company, Assiut, Egypt; eng_ashrafnasr@yahoo.com

has become highly necessary for a clean environment. Solar energy has reserved its first position in the non-conventional energy which are available worldwide [1].

The source of all renewable energy is solar radiation. It can be transformed into electrical energy directly or indirectly using photovoltaic (PV) or thermal collectors, as appropriate [2].

The operating temperature of a PV module has a significant impact on its performance. The module converts most of the energy it absorbs into heat, which is typically lost [3]. Only 4–17% of the solar radiation that enters a PV module is typically converted into electricity. This results in the conversion of more than 50% of incident solar energy into heat, which raises the temperature of the PV module. As a result of a lengthy period of thermal stress (also referred to as thermal degradation of the module), the module's temperature rises, which in turn reduces its electrical yield and efficiency [4]. If the array temperature rises beyond the critical daily temperature, the efficiency of PV modules is significantly reduced. As a result, it is essential to keep the modules' temperature below this threshold. It has been shown that a silicon-based PV panel's efficiency can drop by 0.5% for every 1°C increase in temperature [5]. Around 25°C surface temperature is when PV panel efficiency is at its highest under specific circumstances [6]. Therefore, it becomes essential to regulate the operating temperature range by efficiently cooling PV panels. Therefore, selecting a cooling solution could lengthen the lifespan of solar cells and improve their performance and output of power. Figure (1) displays the most popular methods for cooling solar panels.

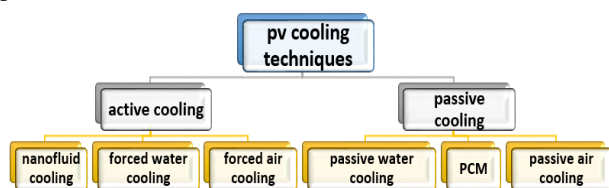


Fig. 1 Most common techniques used for cooling solar PV panels.

1.1. Active cooling

(A). Cooling of PV panels by nanofluids

On the PV's back side (in contact), graphene nanoparticles in a fluid medium can function well as a cooling medium. Through an experimental study, the effective efficiency of cooling PV panels by circulating water around them was increased by 50%. Another

strategy involved putting a PV panel inside a swimming pool at a depth that might lower the temperature from 65°C to 45°C. Nanoparticles range in size from 1 to 100 nm and have a high surface area to volume ratio. These in-water nanoparticles can boost water's ability to conduct heat, speeding up the process of heat transfer. As a result, the cooling might be improved because there would be a lot of nanoparticles. The following describes how the experiment by T.S.Y. Moh et al. [7] was set up: Micro-sized channels are created by melting Poly-dimethyl siloxane (PDMS) at a ratio of 1:10. The experimental study was conducted, and after comparing the outcomes with water as a cooling medium, it was determined that GNP nanofluids cooling exhibits the highest effective efficiency, measured at roughly 42% compared to water cooling with solution being flown at 1.11 L/min flow rate and 54% increase if compared to non-cooling while operating temperature is less than 45°C. Ashij K. Suresha et al. [8] carried out an experimental investigation to determine the efficacy of the nanofluids available on the market, and the following findings are discussed: (1). Al₂O₃ (0.2% by weight), (2) TiO₂, (3). ZnO in deionized water, (4). MgO/water (0.1, 0.2, 0.6% wt.), (5). Polypyrrole, (6). Al₂O₃/water (0.3% wt.) in water as nanofluid at weight fraction of 0.2%, (7). Al₂O₃, CuO with water and Ethylene Glycol (0.1, 0.2, 0.4% wt.). The best results were obtained by Al₂O₃, CuO with water and Ethylene Glycol (0.1, 0.2, 0.4% wt.) with 76.8% increase in thermal efficiency.

(B). Forced water cooling.

Krauter has created a flowing film active water-cooling technique for the PV module surface [9]. Water pouring from the nozzles on the top of the module creates the open-air flowing film on its surface. According to experimental findings, flowing film helped keep the module surface clean and reduced reflection loss by between 2.6 and 3.6 percent. Under the irradiation conditions described in the literature [10], $T_a = 34\text{ }^\circ\text{C}$, $v=1\text{ m/s}$, and a water flow rate from the nozzles of 4.41 L/(min.m²), T_{cell} was lowered to 40 °C ($T_{\text{cell}}=22\text{ }^\circ\text{C}$). The "water trickling method" by Odeh and Behnia [11] has also been presented as an active cooling technique that involves water flowing across the PV module surface. A water trickling tube (diameter: 2.5 cm, module-side length: 65 cm) is fastened to the top of the module on an inclined plane as part of their cooling system. The trickling tube on one side of the module leads to a water-collecting tube on the other, where the open-air water circulates from there. By reflecting sunlight in the water layer, the water flow can aid in module cooling and enhance incident radiation on the

solar cell. As a result of the experiment, T_{cell} was lowered to 32 °C ($T_{\text{cell}} = 26$ °C) with $I = I_{\text{cell}} = 1000$ W/m² and a 4 L/min water flow rate.

(C). Forced air cooling

Mazon-Hern and others investigated forced convection cooling by utilizing fans to cool the PV modules' backs that were positioned on roofs, as shown in Figure (2). When maximum cell temperature decreased by 15 C, the total efficiency increased by 2%. It has been established that the P.V. performance is more influenced by the distance between the module and the roof, the air flow rate, and the local ambient temperature. P.V. systems are not actively cooled by air because they typically stand outside. Due to air movement, the distance between panels is crucial for both system balance and panel cooling [12].



Fig. 2 Air cooling techniques: (A) Natural, (B) Forced.

Erhan Arslan et al. [13] used computational fluid dynamics (CFD) testing on a monocrystalline photovoltaic thermal collector panel and air as the cooling medium through the newly designed copper fin's structure to conduct an energy and exergy study of a unique PV panel. By varying the radial speed of the fans, the air is sucked at various mass flow rates, and an outlet is provided on the upper side of the slanted PV panel. Two different fan speeds were used throughout the testing, resulting in mass flow rates of 0.04553 kg/s and 0.031087 kg/s, respectively. Higher mass flow rates produced more heat transfer, in accordance with the rules of conduction and heat transfer. As illustrated in

Figure (3), this results in more effective cooling of the panel.

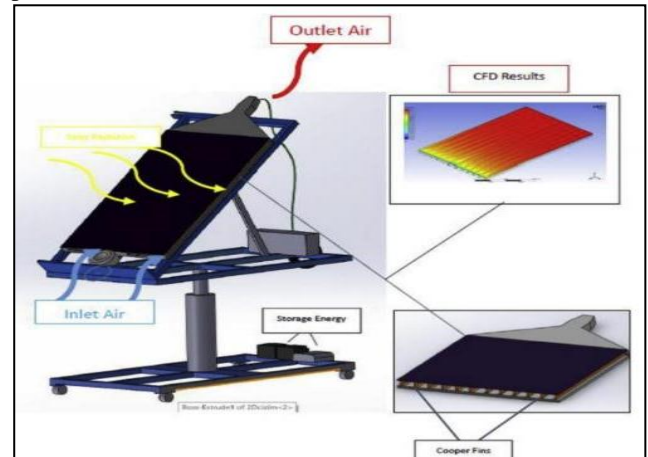


Fig. 3 PV panel cooling using fans [13].

1.2. Passive cooling

(A). passive water cooling

PV modules are submerged when an immersion cooling approach is used. Results for high-efficiency improvement are attained by using water from the PV panels to absorb heat. Immersion of the module in water can enhance performance. Figure (4) from Mehrotra et al.'s study [14] demonstrates how a depth of 1 cm can result in an increase in electrical efficiency of 17.8%. Immersion cooling can potentially reduce high temperatures and has a very low environmental impact; however, it cannot be used with floating solar systems.



Fig. 4 Liquid immersion cooling of PV panels [14].

(B). Passive Phase-change materials (PCM)

When phase change occurs, photovoltaic thermal systems (PVT) with phase-change materials (PCM) can benefit from storage. Along with air and water as the

presumed coolants for the cooling application, phase change materials (PCM) like paraffin wax have also been taken into consideration in PVPCM passive based cooling applications. Experimental research was done to determine how PCM deployment affected an air-cooled solar system's performance. These phase-change materials can assist in absorbing heat from an absorber-plate-covered air channel. Effects of PCM were discussed using a setup that was made available and included a PCM sheet for the PVT.

(C). Passive air cooling

Grubišić et al. [15] carried out a real-world experiment and built two modules to cool the PV solar cell using fans. The first module has metal fans attached to the back surface of the cell longitudinally and regularly, as shown in Figure (5-a), while the second module has aluminum fans attached randomly and erratically, as shown in Figure (5-b). The results showed that the second module produces better outcomes than the first since it was able to increase the cell's efficiency by 2%.

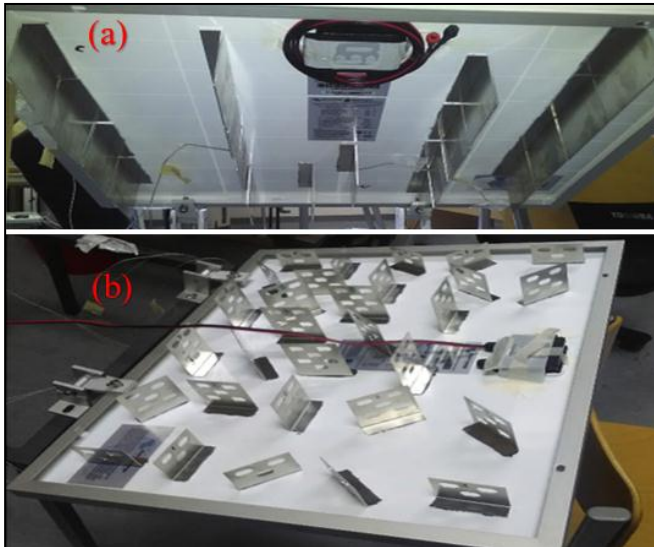


Fig. 5 A photograph of modules belongs to Grubišić et al. [15]

2 Mathematical Models of Solar PV Cell/Module

The single-diode model (SDM), double-diode model (DDM), and PV modules are mathematically modeled in detail in this part, along with the equations required to construct efficient PV models. According to the literature, SDM is straightforward and accurate, but DDM is utilized to increase accuracy.

Figure (6-A) demonstrates the equivalent circuit of

SDM solar PV cell which consists of 1) current source, whose values is dependent on the value of solar radiation, the temperature of the cell, and the characteristics of semiconductor materials; 2) a parallel-resistance, which refers to the spillage of current; 3) diode (D) which mathematically replace the physical effect of P-N junction of the parallel semiconductor material and the current source, where the diode characteristics depend on temperature and load; and 4) series-resistance (R_s) which represents the power losses in the semiconductor [16 - 18].

Kirchhoff's law is used to express the output current I in the SDM equivalent circuit as follows:

$$I = I_{pv} - I_D - \left(\frac{V + I R_s}{R_p} \right) \quad (1)$$

where; I_D and I_{PV} : are diode photo-generated currents respectively in Ampere (A); R_s : series resistance in ohms (Ω); R_p : shunt/parallel resistance in ohms (Ω).

The supply current I_{pv} is linked with a parallel diode D of current I_d which is defined by Shockley formula as [16, 19]:

$$I_D = I_0 \left[\text{Exp} \left(\frac{V + I R_s}{n V_t} \right) - 1 \right] \quad (2)$$

where, n : depends on the design of the semiconductor material fabrication and is called the diode ideality factor; V_t : the thermal voltage in Volt (V) and can be easily obtained from [20, 21]:

$$V_t = \frac{N_s k T}{q} \quad (3)$$

where; T : the panel temperature in Kelvin; k : Boltzmann constant which is equal 1.380649×10^{-23} in Joule/Kelvin; N_s : number of series cells; q : charge of the electron which is equals to $1.602176634 \times 10^{-19}$ in Coulomb. In order to determine the output current, I of the SDM, Eq. (2) must be substituted for Eq. (1) as:

$$I = I_{pv} - I_0 \left[\text{Exp} \left(\frac{V + I R_s}{n V_t} \right) - 1 \right] - \left(\frac{V + I R_s}{R_p} \right) \quad (4)$$

The output current I is defined as follows for the solar PV module, which is made up of numerous parallel strings (N_p) and numerous series cells (N_s), as illustrated in Figure 6-C:

$$I = I_{pv} N_p - I_0 N_p \left[\text{Exp} \left(\frac{\left(\frac{V}{N_s} + \frac{I R_s}{N_p} \right)}{n V_t} \right) - 1 \right] - \left[\frac{\left(\frac{V N_p}{N_s} + I R_s \right)}{R_p} \right] \quad (5)$$

The five unknown parameters that make up the model are summed together in the following equation:

$$\xi = [I_{pv}, I_0, n, R_s, R_p] \quad (6)$$

Figure 6-b shows the double-diode model (DDM), which is similar to the SDM but different in that it has two diodes, D_1 and D_2 , linked in parallel with a current source [22 - 27]. The DDM model is more precise at describing the P-N junction's physical phenomena at low sun brightness levels. The first diode displays the junction's diffusion current, and the other diode is used to monitor recombination effects at the space-charge region. Because there are more parameters in this model than in SDM, it is more complicated.

Kirchhoff's law is used to express the current I in the circuit shown in Figure 6-b as follows:

$$I = I_{pv} - I_{D1} - I_{D2} - \left(\frac{V + I R_s}{R_p} \right) \quad (7)$$

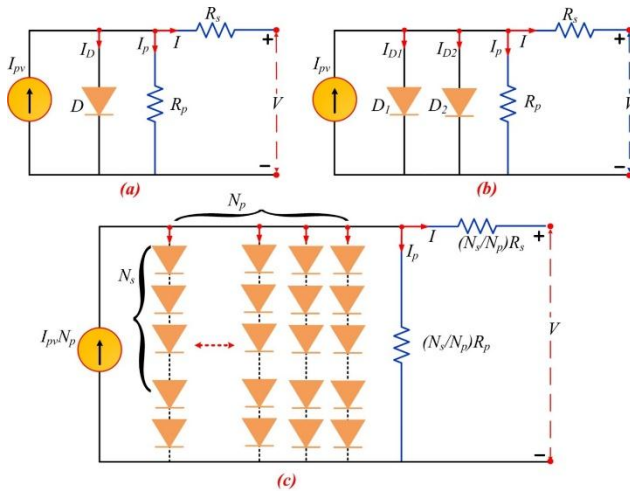


Fig. 6 Equivalent circuit of (a) single-diode model (SDM) (b) double-diode model (DDM), and (c) single-diode model (SDM) based solar PV module.

Where, are the currents passing through diodes D_1 and D_2 are symbolled by I_{D1} and I_{D2} in the equation. The Shockley equation describes them as [16, 28]:

$$I_{D1} = I_{01} \left[\text{Exp} \left(\frac{V + I R_s}{n_1 V_t} \right) - 1 \right] \quad (8)$$

$$I_{D2} = I_{02} \left[\text{Exp} \left(\frac{V + I R_s}{n_2 V_t} \right) - 1 \right] \quad (9)$$

where n_1 and n_2 are D_1 and D_2 ideality factors. The output current I of DDM is obtained by substituting Eqs. (8) and (9) in Eq. (7):

$$I = I_{pv} - I_{01} \left[\text{Exp} \left(\frac{V + I R_s}{n_1 V_t} \right) - 1 \right] - I_{02} \left[\text{Exp} \left(\frac{V + I R_s}{n_2 V_t} \right) - 1 \right] - \left(\frac{V + I R_s}{R_p} \right) \quad (10)$$

It is clear from the previous Eq. 10 that seven unknown parameters must be estimated in order to effectively model DDM. They are condensed into the equation below:

$$\xi = [I_{pv}, I_{01}, I_{02}, n_1, n_2, R_s, R_p] \quad (11)$$

Both SDM and DDM's unknown parameters can be found analytically, numerically, or by utilizing any optimization algorithm.

3 Problem Formulation

The primary goal of the proposed work is to use mathematical modeling and experimental data of the I-V curve for solar PV cells and modules under a variety of temperature and sun brightness conditions to estimate the unknown parameters of SDM and DDM of Eqs. (6) and (11). The primary goal of this method is to reduce the discrepancy between the experimental data and the estimates, as shown in the following equations [18, 22, 24–27, 29, 30]:

Absolute error (AE):

$$AE = \sum_{i=1}^N |I_i - \bar{I}_{(V_i, \xi)}| \quad (12)$$

Mean absolute error (MAE):

$$MAE = \frac{1}{N} \sum_{i=1}^N |I_i - \bar{I}_{(V_i, \xi)}| \quad (13)$$

Root mean square error (RMSE):

$$RMSE = \sqrt{\frac{1}{N} \sum_{i=1}^N (I_i - \bar{I}_{(V_i, \xi)})^2} \quad (14)$$

where, N : is the set of empirical points (I_i, V_i) measured with an index of i ; $\bar{I}_{(V_i, \xi)}$: is the estimated value as a function of the unknown parameters ξ which are characterized by Eqs. (6) and (11).

The objective function (OF) is a function that evaluates the degree of correspondence between the set of parameters that describe the model (each within a specific range) and the exploratory data.

Since RMSE measures the discrepancy between measured and estimated values, OF in this study is RMSE.

The goal of the task is to reduce the difference between the measured data and the estimated parameters of the model, which is stated as:

$$\min(RMSE) = \min \sqrt{\frac{1}{N} \sum_{i=1}^N (I_i - \bar{I}_{(V_i, \xi)})^2} \quad (15)$$

Theoretically, when the precise parameter estimations are obtained, OF should be zero. The level of correspondence depends only on the trial data because the models are heavily predetermined and no information is available regarding the precise estimations of the model parameters. As a result, each drop in the OF (RMSE) value is significant since it indicates that the author is becoming more knowledgeable about the real estimates of the parameters.

3.1. Single-diode model

By comparing the current values that result in the least amount of error, the ideal values of the five unknown parameters, as illustrated in Figure 5-A, are determined. However, because Eq. (6) does not permit a clear organization, there is a significant barrier to both parameterizing the model and recreating it. Numerical techniques, such as the Newton-Raphson method (NRM) or the bisection method (BM), can be used to get around this restriction [31, 32].

So, NRM is used to obtain $(\bar{I}_{(V_i, \xi)})$ the estimated current, whose flowchart is demonstrated in Figure 7, the value of the function $f(\bar{I}_{(V_i, \xi)})$, successively, until achieving the halting condition, $|f(\bar{I}_{(V_i, \xi)})| < 10^{-10}$. To compute the updated estimation of the evaluated current $\bar{I}_{(V_i, \xi)}$, information on the derivative of the function $f(\bar{I}_{(V_i, \xi)})$ concerning $\bar{I}_{(V_i, \xi)}$ are required as expressed as [33, 34]:

$$f(\bar{I}_{(V_i, \xi)}) = I_{ph} - I_0 \left[e^{\frac{V + \bar{I}_{(V_i, \xi)} R_s}{n V_t}} - 1 \right] - \left(\frac{V_i + \bar{I}_{(V_i, \xi)} R_s}{R_p} \right) - \bar{I}_{(V_i, \xi)} \quad (16)$$

$$\frac{\partial f(\bar{I}_{(V_i, \xi)})}{\partial \bar{I}_{(V_i, \xi)}} = - \left(\frac{I_0 R_s e^{\frac{V + \bar{I}_{(V_i, \xi)} R_s}{n V_t}}}{n V_t} - \left(\frac{V_i + \bar{I}_{(V_i, \xi)} R_s}{R_p} \right) \right) - \frac{R_s}{R_p} - 1 \quad (17)$$

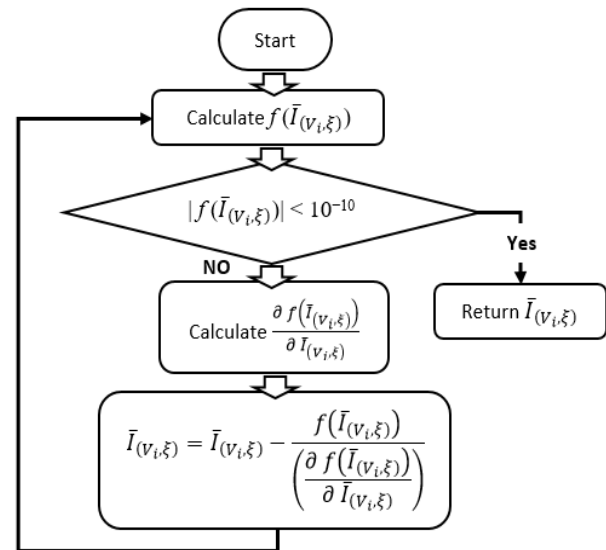


Fig. 7 Flowchart of the Newton-Raphson method (NRM).

3.2. Double-diode model

The best estimates of the seven elusive parameters, as illustrated in Figure 6-b, are obtained by evaluating the current characteristics that result in the fewest errors. Similar to the preceding model, the extracted current $\bar{I}_{(V_i, \xi)}$ is likewise derived using NRM, whose flowchart is given in Figure 6, and with Eqs. (16) and (17) being substituted by the subsequent equations [35,36]:

$$f(\bar{I}_{(V_i, \xi)}) = I_{ph} - I_{01} \left[e^{\frac{V + \bar{I}_{(V_i, \xi)} R_s}{n_1 V_t}} - 1 \right] - I_{02} \left[e^{\frac{V + \bar{I}_{(V_i, \xi)} R_s}{n_2 V_t}} - 1 \right] \quad (18)$$

$$\frac{\partial f(\bar{I}_{(V_i, \xi)})}{\partial \bar{I}_{(V_i, \xi)}} = - \left(\frac{I_{01} R_s e^{\frac{V + \bar{I}_{(V_i, \xi)} R_s}{n_1 V_t}}}{n_1 V_t} - \left(\frac{V_i + \bar{I}_{(V_i, \xi)} R_s}{R_p} \right) \right) - \left(\frac{I_{02} R_s e^{\frac{V + \bar{I}_{(V_i, \xi)} R_s}{n_2 V_t}}}{n_2 V_t} - \left(\frac{V_i + \bar{I}_{(V_i, \xi)} R_s}{R_p} \right) \right) - \frac{R_s}{R_p} - 1 \quad (19)$$

4 Experimental Set-Up

This work aims to study and investigate the effect of cooling PV panels using different cooling techniques on the performance of solar PV panels. At Assiut University in Egypt, this investigation was carried out in the Renewable Energy Laboratory. In order to assure optimal energy output throughout the year, the PV

panels have been installed on the roof of the laboratory with a tilt angle of 30° , facing south, consistent with the site's latitude. Before the readings, all PV panels were kept clean. Results were recorded for a period of 6-weeks, starting from first of September to the middle of October 2022, they were monitored every hour from 8:00 am to 5:00 pm. Practically, to study the most effect of cooling techniques of PV cells. four identical PV panels are used in this study but with different cooling techniques, first one is a reference panel (Panel A), second one which using water spray technique (Panel B), third one which using iron-serpentine with water technique (Panel C) and the fourth one which using fame-glass technique (Panel D), as shown in Figures 8 through 11.



Fig. 8 PV panels with different cooling techniques, (A) Reference panel; (B) Water-spray technique; (C) Iron-serpentine with water technique; and (D) Fame-glass technique.

Panel A: Reference Panel which did not use any cooling technique with it, to study the effect of cooling techniques on other PV panels, Figure 8-a.

Panel B: Water-spray technique for cooling PV Panels which is using a spray system, as shown in Figures 8-b and 9, to spray water over the Panel for 5 minutes and stopped for 10 minutes. This process is repeated all day from 8:00 am to 5:00 pm.

Panel C: Iron-serpentine with water technique which is used to cool the PV panel by using a serpentine made from iron installed in the back site of the panel with water passing through it to cool the panel, as shown in Figures 8-c and 10. Water flows inside the serpentine all the working hours of the cell without stopping, from 8:00 am to 5:00 pm.

Panel D: Fame-glass technique which uses a separate fame-glass which is placed slightly higher than the PV panel as shown in Figures 8-d and 11.

During a period of 6-weeks, results of panel voltage (V), current (I), temperatures (T °C) and solar irradiation (W/m^2) were monitored and recorded every hour from 8:00 am to 5:00 pm, tools which are used for measuring are shown in Figure 12.



Fig. 9 Technique of the water-spray system for cooling PV Panels (Panel B).



Fig. 10 Iron-serpentine with water technique for cooling PV Panels (Panel C).



Fig. 11 Fame-glass technique for cooling PV Panels (Panel D).



Fig. 12 Tools used for measuring panel voltage, current, temperature and radiation of PV panels; Renewable Energy Laboratory at Assiut University, Egypt.

5 Results and discussions

Figures from 12 to 20 show the I-V and P-V curves of the four panels under the study; black curves represent recording measurements of reference panel (Panel A) which is not using any cooling techniques, red curves represent recording measurements of panel using spray water technique (Panel B), blue curves represent recording measurements of panel using iron-serpentine with water technique (Panel C) and finally purple curves represent recording measurements of panel using fame-glass technique (Panel D).

Figure 13 shows the experimental results of I-V and P-V curves using different cooling techniques of same PV panels on September 15th, 2022; 9 AM; SR = 797 W/m²; T = 45° C; Renewable Energy Laboratory at Assiut University, Egypt. The efficiency of panel using spray-water technique (panel B) increases by about 1 % more than reference panel (Panel A), the efficiency of panel using serpentine with water technique (panel C) increases by about 1.6 % more than reference panel (Panel A), and the efficiency of panel using fame-glass technique (Panel D) decreases by about 71 % less than reference panel (Panel A). These results observe that in a low temperature and low solar irradiation at early

morning, there is a little effect of cooling in performance of panels ,also fame-glass technique of cooling has a negative effect.

Figure 14 shows the experimental results of I-V and P-V curves using different cooling techniques of same PV panels on September 15th, 2022; 10 AM; SR = 1070 W/m²; T = 47.5 °C; Renewable Energy Laboratory at Assiut University, Egypt. The efficiency of panel using spray-water technique (panel B) increases by about 2 % more than reference panel (Panel A), the efficiency of panel using serpentine with water technique (panel C) increases by about 20 % more than reference panel (Panel A), and the efficiency of panel using fame-glass technique (Panel D) decreases by about 40 % less than reference panel (Panel A). When radiation and temperature increased, cooling effect increased, and the total efficiency of solar panel performance is better. Also, with increasing radiation and temperature, negative effect fame-glass technique of cooling is partially improved, but still negative due to the shading phenomenon.

Figure 15 shows the experimental results of I-V and P-V curves using different cooling techniques of same PV panels on September 15th, 2022; 11 AM; SR = 1132 W/m²; T = 48.2° C; Renewable Energy Laboratory at Assiut University, Egypt. The efficiency of panel using spray-water technique (panel B) increases by about 17 % more than reference panel (Panel A), the efficiency of panel using serpentine with water technique (panel C) increases by about 13 % more than reference panel (Panel A), and the efficiency of panel using fame-glass technique (Panel D) decreases by about 42 % less than reference panel (Panel A).

Figure 16 shows the experimental results of I-V and P-V curves using different cooling techniques of same PV panels on September 15th, 2022; 12 PM; SR = 1070 W/m²; T = 50.7 °C; Renewable Energy Laboratory at Assiut University, Egypt. The efficiency of panel using spray-water technique (panel B) increases by about 23 % more than reference panel (Panel A), the efficiency of panel using serpentine with water technique (panel C) increases by about 22 % more than reference panel (Panel A), and the efficiency of panel using fame-glass technique (Panel D) decreases by about 34 % less than reference panel (Panel A).

Figure 17 shows the experimental results of I-V and P-V curves using different cooling techniques of same PV panels on September 15th, 2022; 1 PM; SR = 1070 W/m²; T = 50 °C; Renewable Energy Laboratory at Assiut University, Egypt. The efficiency of panel using spray-water technique (panel B) increases by about 12 % more than reference panel (Panel A), the efficiency of panel using serpentine with water technique (panel C)

increases by about 2 % more than reference panel (Panel A), and the efficiency of panel using fame-glass technique (Panel D) decreases by about 52 % less than reference panel (Panel A).

Figure 18 shows the experimental results of I-V and P-V curves using different cooling techniques of same PV panels on September 15th, 2022; 2 PM; SR = 965 w/m²; T = 48.3° C; Renewable Energy Laboratory at Assiut University, Egypt. The efficiency of panel using spray-water technique (panel B) increases by about 20 % more than reference panel (Panel A), the efficiency of panel using serpentine with water technique (panel C) increases by about 24 % more than reference panel (panel A), and the efficiency of panel using fame-glass technique (panel D) decreases by about 37 % less than reference panel (panel A).

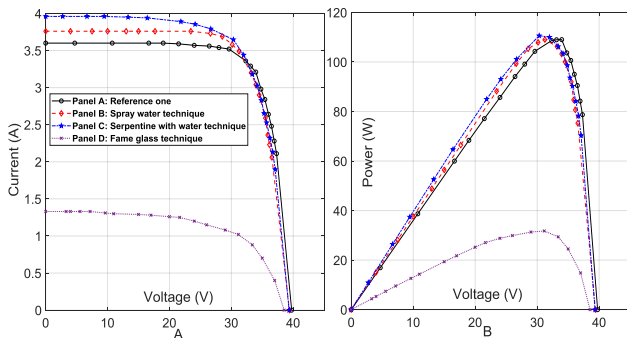


Fig. 13 Experimental results of using different cooling techniques of same PV panels; (A) I-V curve, and (B) P-V curve; (September 15th, 2022; 9 AM; SR = 797 W/m²; T = 45° C; Assiut University, Egypt).

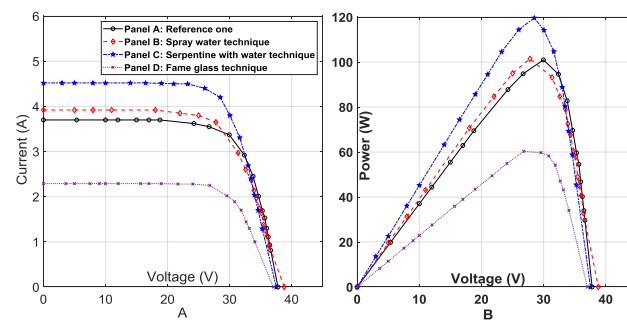


Fig. 14 Experimental results of using different cooling techniques of same PV Panels; (A) I-V cure, and (B) P-V cure; (September 15th, 2022; 10 AM; SR = 1070 W/m²; T = 47.5° C; Assiut University, Egypt).

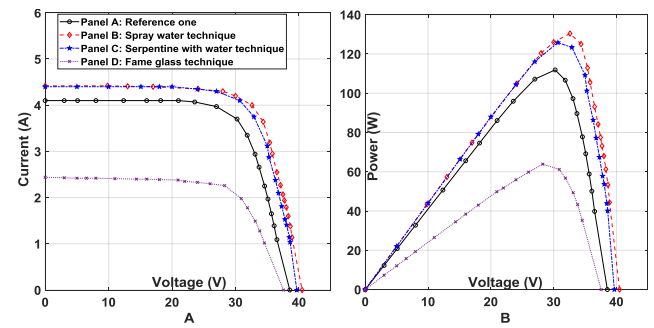


Fig. 15 Experimental results of using different cooling techniques of same PV Panels; (A) I-V cure, and (B) P-V cure; (September 15th, 2022; 11 AM; SR = 1132 w/m²; T = 48.2° C; Assiut University, Egypt).

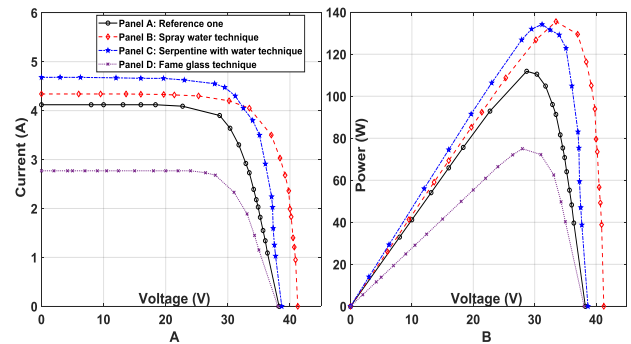


Fig. 16 Experimental results of using different cooling techniques of same PV Panels; (A) I-V cure, and (B) P-V cure; (September 15th, 2022; 12 PM; SR = 1070 W/m²; T = 50.7° C; Assiut University, Egypt).

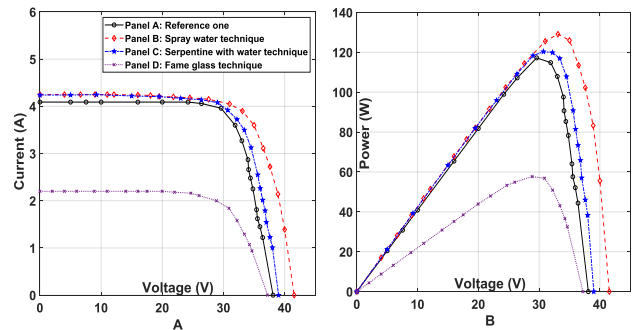


Fig. 17 Experimental results of using different cooling techniques of same PV Panels; (A) I-V cure, and (B) P-V cure; (September 15th, 2022; 1 PM; SR = 1070 W/m²; T = 50 °C; Assiut University, Egypt).

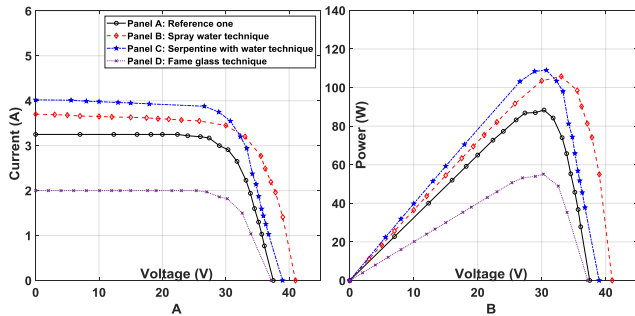


Fig. 18 Experimental results of using different cooling techniques of same PV Panels; (A) I-V cure, and (B) P-V cure; (September 15th, 2022; 2 PM; SR = 965 w/m²; T = 48.3° C; Assiut University, Egypt).

Figure 19 shows the experimental results of I-V and P-V curves using different cooling techniques of same PV panels on October 1st, 2022; 11 AM; SR = 1118 W/m²; T = 51° C; Renewable Energy Laboratory at Assiut University, Egypt. The efficiency of panel using spray-water technique (panel B) increases by about 14 % more than reference panel (Panel A), the efficiency of panel using serpentine with water technique (panel C) increases by about 3 % more than reference panel (Panel A), and the efficiency of panel using fame-glass technique (Panel D) decreases by about 46 % less than reference panel (Panel A).

Figure 20 shows the experimental results of I-V and P-V curves using different cooling techniques of same PV panels on September 15th, 2022; 12 PM; SR = 1136 W/m²; T = 52.5° C; Renewable Energy Laboratory at Assiut University, Egypt. The efficiency of panel using spray-water technique (panel B) increases by about 23 % more than reference panel (Panel A), the efficiency of panel using serpentine with water technique (panel C) increases by about 6 % more than reference panel (Panel A), and the efficiency of panel using fame-glass technique (Panel D) decreases by about 31 % less than reference panel (Panel A).

Figure 21 shows the experimental results of I-V and P-V curves using different cooling techniques of same PV panels on October 1st, 2022; 4 PM; SR = 700 w/m²; T = 45° C; Renewable Energy Laboratory at Assiut University, Egypt. The efficiency of panel using spray-water technique (panel B) increases by about 0.1 % more than reference panel (Panel A), the efficiency of panel using serpentine with water technique (panel C) increases by about 1.45 % more than reference panel (Panel A), and the efficiency of panel using fame-glass technique (Panel D) decreases by about 70 % less than reference panel (Panel A). At the end-hours of the day, with a low temperature and low solar irradiation, also there is a little effect of cooling in the performance of panels. Using Serpentine with water technique (Panel C)

for cooling of solar PV panels with low temperatures is better than other techniques, Figures 12 and 20.

At high temperatures, cooling by using spray water technique (panel B) is better than cooling by using serpentine with water technique (Panel C), Figures 13, 14, 15, 16, 17, 18 and 19.

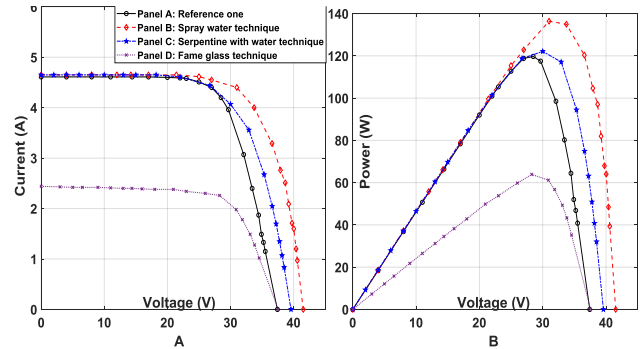


Fig. 19 Experimental results of using different cooling techniques of same PV Panels; (A) I-V cure, and (B) P-V cure; (October 1st, 2022; 11 AM; SR = 1118 W/m²; T = 51° C; Assiut University, Egypt).

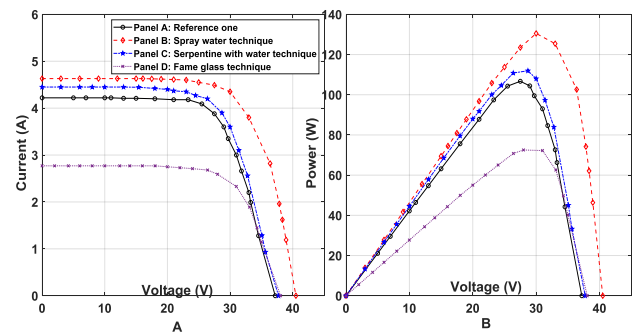


Fig. 20 Experimental results of using different cooling techniques of same PV Panels; (A) I-V cure, and (B) P-V cure; (October 1st, 2022; 12 PM; SR = 1136 W/m²; T = 52.5° C; Assiut University, Egypt).

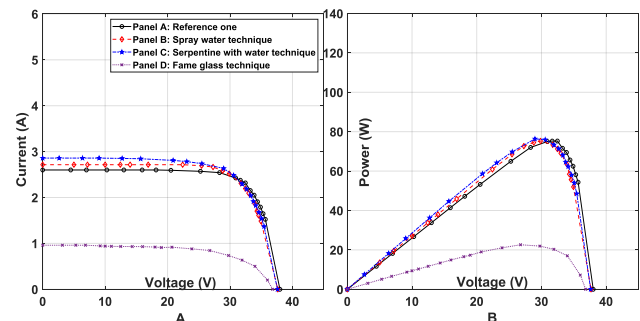


Fig. 21 Experimental results of using different cooling techniques of same PV Panels; (A) I-V curve, and (B) P-V curve; (October 1st, 2022; 4 PM; SR = 700 W/m²; T = 45° C; Assiut University, Egypt).

Figure 22 shows thermal effect resulting of different cooling techniques of PV Panels on September 15th,

2022; 12:55 PM; SR = 1070 W/m²; T = 50° C; Renewable Energy Laboratory at Assiut University, Egypt. Temperatures are high on reference panel (panel A) as exceeding 55° C then it is decreased using different cooling techniques, spraying water techniques (panel B), iron-serpentine techniques (panel C) and fame-glass techniques (panel D).

Figure 23 shows the experimental I-V curve results of using different cooling techniques of same PV Panels; reference panel, water spray technique, iron serpentine technique and, fame glass technique; Renewable Energy Laboratory at Assiut University, Egypt.

Figure 23 shows the experimental output power of solar PV panels during daytime using different cooling techniques; reference panel, water spray technique, iron serpentine technique and, fame glass technique; Renewable Energy Laboratory at Assiut University, Egypt.

Figure 24 shows a comparison of output power of solar PV panels during daytime using different cooling techniques at different temperatures; reference panel, water spray technique, iron serpentine technique and, fame glass technique; Renewable Energy Laboratory at Assiut University, Egypt.

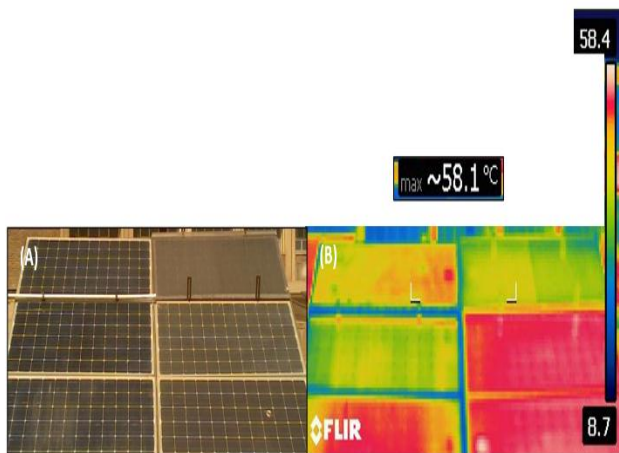


Fig. 22 Thermal effect resulting of different cooling techniques of PV Panels; (A) normal picture and (B) thermal picture. (September 15th, 2022; 12:55 PM; SR = 1070 W/m²; T = 50 °C; Assiut University, Egypt).

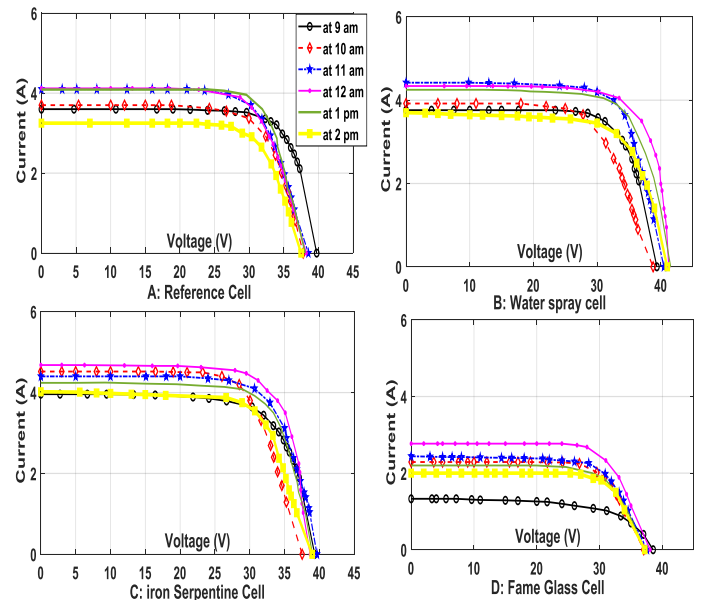


Fig. 23 Experimental I-V curve results of using different cooling techniques of same PV Panels; (A) Reference panel, and (B) Water spray technique, (C) Iron serpentine technique and, (D) Fame glass technique; Assiut University, Egypt. (September 15th, 2022; 12:55 PM; SR = 1070 W/m²; T = 50° C; Assiut University, Egypt).

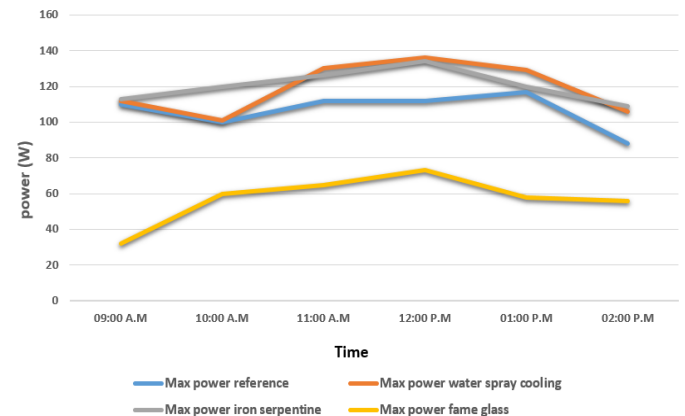


Fig. 24 Experimental output power of solar PV panels during daytime using different cooling techniques; (A) Reference panel, and (B) Water spray technique, (C) Iron serpentine technique and, (D) Fame glass technique; Assiut University, Egypt.

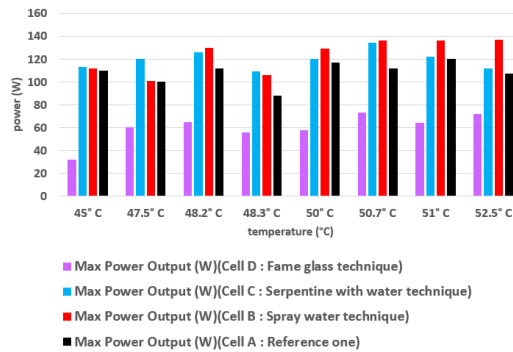


Fig. 25 Comparison of output power of solar PV panels during daytime using different cooling techniques at different temperatures; Experimental (A) Reference panel, and (B) Water spray technique, (C) Iron serpentine technique and, (D) Fame glass technique; Assiut University, Egypt.

6 Conclusions

At a low temperature and low solar irradiation, early morning and end-hours of the day, there is little effect of cooling in efficiency and performance of panels. When radiation and temperature increased, cooling effect increased, and the total efficiency and performance of panels is better. At high temperatures, cooling by using spray water technique (panel B) is better than cooling by using serpentine with water technique (Panel C) while Fame-glass technique of cooling has a negative effect.

With increasing radiation and temperature, negative effect fame-glass technique of cooling is partially improved, but still negative due to the shading phenomenon. At low temperatures, using Serpentine with water technique (Panel C) for cooling of solar PV panels with is better than using spray water technique (panel B). Note that it rarely happens at high temperatures that the cooling effect of using Serpentine with water technique (Panel C) is better than using spray water technique (panel B), and this is often due to the shading phenomenon when the results is monitored during the spraying process.

References

[1] Palacios, A., et al. "Thermal energy storage technologies for concentrated solar power—A review from a materials perspective." *Renewable Energy* 156 (2020): 1244-1265.

[2] Pandey, Adarsh Kumar, Reji Kumar, and M. Samyano. "Solar energy: direct and indirect methods to harvest usable energy." *Dye-Sensitized Solar Cells*. Academic Press, 2022. 1-24.

[3] H. Bahaidarah, A. Subhan, P. Gandhidasan, S. Rehman, Performance evaluation of a PV (photovoltaic) module by

back surface water cooling for hot climatic conditions, *Energy* 59 (Sep) (2013) 445–453.

[4] M. Chandrasekar, S. Suresh, T. Senthilkumar, M. Ganesh karthikeyan, Passive cooling of standalone flat PV module with cotton wick structures, *Energy Convers. Manage.* 71 (Jul) (2013) 43–50.

[5] Negin Choubineh, Hamid Jannesari and Alibakhsh Kasaeian, Experimental study of the effect of using phase change materials on the performance of an air-cooled photovoltaic system, *Renewable and Sustainable Energy Reviews*, Volume 101, March 2019, Pages 103-111

[6] Nethra MR and Kalidasan B, Earth tube heat exchanger design for efficiency enhancement of PV panel, *MaterialsToday: Proceedings*, Volume 45, Part 2, 2021, Pages 587-591

[7] T.S.Y. Moh, T.W.Ting and A.H.Y. Lau, Graphene Nanoparticles (GNP) nanofluids as key cooling media on a flat solar panel through micro-sized channels, *Energy Reports*, Volume 6, Supplement 2, February 2020, Pages 282-286

[8] Ashij K. Suresha, Sahil Khurana, Gopal Nandan, Gaurav Dwivedi and Satish Kumar, Role on nanofluids in cooling solar photovoltaic cell to enhance overall efficiency, *MaterialsToday: Proceedings*, Volume 5, Issue 9, Part 3, 2018, Pages 20614-20620

[9] Krauter S. Increased electrical yield via water flow over the front of photovoltaic panels. *Sol Energy Mater Sol Cells* 2004;82:131–7.

[10] Schmid U. Thermische und optische optimierung von PV-modulen mittels aktiver wasserkühlung zur verbesserung des wirkungsgrades [Master thesis]. Germany: Institute of Electrical Energy Technology, Technical University Berlin; 1999.

[11] Odeh S, Behnia M. Improving photovoltaic module efficiency using water cooling. *Heat Transf Eng* 2009;30: 499–505.

[12] R. Mazón-Hernández, J. R. García-Cascales, F. Vera-García, A. S. Káiser, and B. Zamora., "Improving the Electrical Parameters of a Photovoltaic Panel by Means of an Induced or Forced Air Stream", February 2013, *International Journal of Photoenergy*, Vol. 2013, p. 10

[13] Erhan Arslan, Mustafa Aktaş and Ömer Faruk Can, Experimental and numerical investigation of a novel photovoltaic thermal (PV/T) collector with the energy and exergy analysis, *Journal of Cleaner Production*, Volume 276, 10 December 2020, 123255

[14] S. Mehrotra S, P. Rawat, M. Debbarma, K. Sudhakar, Performance of a solar panel with water immersion cooling technique, *Int. J. Sci. Environ. Technol.* 3 (2014) 1161–1172.

[15] Grubišić-Čabo F, Nižetić S, Čoko D, Marinić Kragić I, Papadopoulos A (2018) Experimental investigation of the passive cooled free-standing photovoltaic panel with fixed aluminum fins on the backside surface. *J Clean Prod* 176:119–129. <https://doi.org/10.1016/j.jclepro.2017.12.149>

[16] Rezk, H.; Ziedan, H.A.; Abd-Elbary, H.; Alamri, H.R.; Elnozahy A. Experimental Investigation to Improve the Energy Efficiency of Solar PV Panels Using Hydrophobic SiO₂ Nanomaterial. *Coatings* 2020, 10(5), 503. Doi: 10.3390/coatings10050503

[17] Muhammad, F.F.; Sangawi, A.W.K.; Hashim, S.; Ghoshal, S.K.; Abdullah, I.K.; Hameed, S.S. Simple and efficient estimation of photovoltaic cells and modules parameters using approximation and correction technique. *PLOS ONE* 2019, 14 (5): e0216201. Doi: 10.1371/journal.pone.0216201

- [18] Hsieh, Y.-C.; Yu, L.-R.; Chang, T.-C.; Liu, W.-C.; Wu, T.-H.; Moo, C.-S. Parameter Identification of One-Diode Dynamic Equivalent Circuit Model for Photovoltaic Panel. *IEEE Journal of Photovoltaics* 2019. DOI: 10.1109/JPHOTOV.2019.2951920
- [19] Mohamed, M.A.; Diab, A.A.Z.; Rezk, H. Partial shading mitigation of PV systems via different meta-heuristic techniques. *Renewable Energy* 2019, 130, 1159-1175. Doi: 10.1016/j.renene.2018.08.077
- [20] Xu, S.; Wang, Y. Parameter estimation of photovoltaic modules using a hybrid flower pollination algorithm. *Energy Conversion and Management* 2017, 144, 53-68. Doi: 10.1016/j.enconman.2017.04.042
- [21] Yu, K.; Liang, J.J.; Qu, B.Y.; Chen, X.; Wang, H. Parameters identification of photovoltaic models using an improved JAYA optimization algorithm. *Energy Conversion and Management* 2017, 150, 742-753. Doi: 10.1016/j.enconman.2017.08.063
- [22] Nunes, H.G.; Pombo, J.N.; Bento, P.R.; Mariano, S.P.; Calado, M.A. Collaborative swarm intelligence to estimate PV parameters. *Energy Conversion and Management* 2019, 185, pp. 866-890. Doi: 10.1016/j.enconman.2019.02.003
- [23] Sabudin, S.N.; Jamil, N.M. Parameter Estimation in Mathematical Modelling for Photovoltaic Panel. *International Conference on Science and Innovated Engineering (I-COSINE)*, IOP Conf. Series: Materials Science and Engineering 2019, 536, 012001, pp. 1-11. Doi:10.1088/1757-899X/536/1/012001
- [24] Nunes, H.G.; Pombo, J.N.; Mariano, S.P.; Calado, M.A.; Souza, J.F. A new high performance method for determining the parameters of PV cells and modules based on guaranteed convergence particle swarm optimization. *Applied Energy* 2018, 211, pp. 774-791. Doi: 10.1016/j.apenergy.2017.11.078
- [25] Xiong, G.; Zhang, J.; Yuan, X.; Shi, D.; He, Y.; Yao, G. Parameter estimation of solar photovoltaic models by means of a hybrid differential evolution with whale optimization algorithm. *Solar Energy* 2018, 176, 742-761. Doi: 10.1016/j.enconman.2018.08.053
- [26] Kang, T.; Yao, J.; Jin, M.; Yang, S.; Duong, T. A Novel Improved Cuckoo Search Algorithm for Parameter Estimation of Photovoltaic (PV) Models. *Energies* 2018, 11, 1060. Doi: 10.3390/en11051060
- [27] Gao, X.; Cui, Y.; Hu, J.; Xu, G.; Wang, Z.; Qu, J.; Wang, H. Parameter extraction of solar cell models using improved shuffled complex evolution algorithm. *Energy Conversion and Management* 2018, 157, pp. 460-479. Doi: 10.1016/j.enconman.2017.12.033
- [28] Jadli, U.; Thakur, P.; Shukla, R.D. A New Parameter Estimation Method of Solar Photovoltaic. *IEEE Journal of Photovoltaics* 2018, 8 (1), pp. 239-247. Doi: 10.1109/JPHOTOV.2017.2767602
- [29] Elazab, O.S.; Hasanien, H.M.; Alsaidan, I.; Abdelaziz A.Y.; Mueeen, S.M. Parameter Estimation of Three Diode Photovoltaic Model Using Grasshopper Optimization Algorithm. *Energies* 2020, 13, 497; Doi: 10.3390/en13020497
- [30] Qais, M.H.; Hasanien, H.M.; Alghuwainem, S. Identification of electrical parameters for three-diode photovoltaic model using analytical and sunflower optimization algorithm. *Applied Energy* 2019, 250, pp. 109-117. Doi:10.1016/j.apenergy.2019.05.013
- [31] Jordehi, A.R. Time varying acceleration coefficients particle swarm optimisation (TVACPSO): a new optimisation algorithm for estimating parameters of PV cells and modules. *Energy Convers Manage* 2016, 129:262-74. Doi: 10.1016/j.enconman.2016.09.085
- [32] Rezk, H.; Fathy, A. A novel optimal parameters identification of triple-junction solar cell based on a recently meta-heuristic water cycle algorithm. *Solar Energy* 2017, 157, 778-791. Doi: 10.1016/j.solener.2017.08.084
- [33] Rezk, H.; Aly, M.; Al-Dhaifallah, M.; Shoyama, M. Design and Hardware Implementation of New Adaptive Fuzzy Logic-Based MPPT Control Method for Photovoltaic Applications. *IEEE Access* 2019, 7, 106427-106438. Doi: 10.1109/ACCESS.2019.2932694
- [34] Ibrahim, M.N.; Rezk, H.; Al-Dhaifallah, M.; Sergeant, P. Solar array fed synchronous reluctance motor driven water pump: An improved performance under partial shading conditions. *IEEE Access* 2019, 7, 77100-77115. Doi: 10.1109/ACCESS.2019.2922358
- [35] Abdalla, O.; Rezk, H.; Ahmed E.M. Wind Driven Optimization Algorithm Based Global MPPT for PV System under Non-Uniform Solar Irradiance. *Solar Energy* 2019, 180, 429-444. Doi: 10.1016/j.solener.2019.01.056
- [36] Rezk, H.; Mazen, A.L.O.; Gomaa, M.R.; Tolba, M.A. Fathy, A.; Abdelkareem, M.A. A novel statistical performance evaluation of most modern optimization-based global MPPT techniques for partially shaded PV system. *Renewable and Sustainable Energy Reviews* 2019, 115, 109372. Doi: 10.1016/j.rser.2019.109372